



MAXIMUM POWER TRACKING TECHNIQUE FOR DOUBLY FED INDUCTION GENERATOR (DFIG)-BASED WIND TURBINES

P.SAMYUKTHA

Assistant Professor, Dept Of EEE, Nishitha College Of Engineering And Technology, Kandukur, RR-DIST, Hyderabad, TS, India.

S.SRIVIDYA

PG Scholar, Dept Of EEE(PE), Nishitha College Of Engineering And Technology, Kandukur, RR-DIST, Hyderabad, TS, India,

Abstract:

The main aim this project is a maximum power tracking technique is presented for doubly fed induction generator (DFIG)-based wind turbines. The recent sensitive issue of climate change is due to the extensive amount of carbon emission through the consumption of fossil fuel as the primary option for energy demand. Due to the negative impact of green house effect, the alternative and renewable energy options have received significant attention global scale. The two branched approach of renewable energy projects including the reduction in the global greenhouse gas emissions and encouragement to the development of alternate green energy options like wind energy. Wind energy has become one of most acceptable solution among the different renewable energy resources because of the application of power electronic based controllers that allows the wind energy conversion system (WECS) to generate quality electric power irrespective of variable wind profile. The continuous flow of quality power from WECS to grid is insured for wider range of wind speed. Doubly fed induction generator (DFIG) used in WECS having power electronic converter which requires very small friction of power in comparison to the total generation capacity. This paper brings out the analysis of a DFIG system in terms of its stator and rotor currents and real and reactive power balance when the machine is operating with varying wind velocity conditions. Various possible maximum power point tracking techniques are listed in the paper. The suitable Maximum power point tracking (MPPT) technique has also been suggested to harness maximum available power for a given wind velocity to ensure the continuous power flow from WECS to the power grid.

Keywords: Wind turbines, DFIG based wind turbines, nonlinear control, and maximum power tracking.

INTRODUCTION

Wind power generation systems based on a doubly fed induction generator (DFIG) have acquired increasing popularity all over the world due to the advantages of smaller converter rating, independent regulation of active and reactive powers, and lower converter cost and power losses compared with the fixed-speed induction generators or synchronous generators with full-sized converters. The control strategy of a DFIG system under an ideal power grid has been well investigated to satisfy the requirements of wind energy conversion and grid code. However, the practical power grid would always contain negative and harmonic voltage components, especially the 5th and 7th harmonic components. Thus, a severely unbalanced and distorted DFIG stator current would be produced. Currently, a grid operator always requires that the current injected by the renewable energy generation system should be balanced and sinusoidal, so that the power grid would not be further polluted.

However, as the ratio of renewable energy including solar energy and wind energy becomes increasingly higher in power supply, the pulsation components of total active and reactive powers generated by the renewable power generation system will also be increasingly higher. This will be a potential threat for the operational stability of power grid frequency and voltage. Even the safe and reliable operation of the power grid and renewable power generation system will be jeopardized. Therefore, to ensure reliable operation of the power grid and renewable energy generation system over the full range of operational conditions, the elimination of instantaneous active and reactive power fluctuation components at twice and six times the grid frequency is also chosen as a control target in this paper. Moreover, the DFIG electromagnetic torque pulsation caused by a non ideal grid voltage would also be harmful to mechanical units, such as the gearbox and rotor bearing. It is essential to improve the DFIG control strategy to eliminate these detrimental influences. Up to now, the control



technique of DFIG under unbalanced grid voltage has been investigated to eliminate the harmful influence of the grid voltage negative sequence, that is, the unbalanced stator current, instantaneous stator active and reactive power pulsations, and electromagnetic torque pulsation.

On the other hand, when grid voltage distortion occurs, have presented a mathematical modeling and control strategy for DFIG under harmonically distorted grid voltage conditions, in which the alternative control targets were proposed to remove harmonically distorted stator current, restrain stator active and reactive power pulsations, or suppress electromagnetic torque pulsation. Furthermore, we investigated the DFIG control strategy under the unbalanced and harmonic grid voltage to achieve the sinusoidal and balanced stator current, eliminate the electromagnetic torque ripple, or eliminate the stator active power pulsation. However, these studies were implemented based on the grid voltage negative and harmonic sequence decomposition. Then the inevitable phase delay and time delay due to the employment of the notch filters and low-pass filters would be introduced as a consequence, and the decomposition accuracy and system dynamic response would also deteriorate. Furthermore the control reference calculation process is complicated and time-consuming. This process will also be unfavorable for digital implementation in practical applications.

To avoid harmonic decomposition and complicated reference calculation, an additional resonant closed-loop control of DFIG stator current was added in Liu *et al.* (2012), which can eliminate the harmonic components of the stator current under the harmonic grid voltage. Because neither harmonic decomposition nor rotor current reference calculation is needed, the dynamic performance of the DFIG system can be enhanced. However, the unbalanced grid condition was not considered in Liu *et al.* (2012), and the control target of smooth output power and smooth torque, which is a considerable factor in the reliable operation of a DFIG system, was also ignored. To enhance the operation performance of DFIG under the condition of both grid voltage unbalance and harmonic distortion, direct power control (DPC) was implemented because of its advantage of DPC capability, simple implementation, and fast dynamic response (Zhou *et al.*, 2009; Nian *et al.*, 2011; Nian and Song, 2014). Moreover, vector oriented control (VOC) is a popular control strategy which has been widely adopted. Future work on improving the conventional VOC strategy can be expected. When DFIG works under the unbalanced

and distorted grid voltage conditions, both conventional VOC and DPC would be inappropriate due to complicated negative and harmonic component extraction, as well as the time-consuming control reference calculation although grid voltage harmonic distortion was considered in the DFIG control based on DPC in Nian and Song (2014), only one control target of smooth active and reactive powers was introduced.

In this paper, the three alternative control targets can be implemented under the unbalanced and harmonic voltage conditions to achieve reliable and stable operation of the DFIG:

Target I: Balanced and sinusoidal stator current to ensure balanced heating and less harmonic loss in the three-phase stator winding, as well as to improve the power quality injected into the power grid.

Target II: Smooth stator active and reactive powers to ensure smooth wind energy injection into the power grid, which would be beneficial to safe and reliable grid operation.

Target III: Smooth electromagnetic torque to ensure reliable operation of the DFIG mechanical component, such as the gearbox and rotor bearing

I. WIND ENERGY CONVERSION SYSTEM (WECS)

Green house gas reduction has been one of the crucial and inevitable global challenges. The issue has come into focus especially in the last two decades as evidences on global warming have been reported. This has drawn increasing attention to renewable energies including wind energy. WECS has annual installation growth rate of 31.7% in 2009 with its growth rate is continuously increasing for the last few years. The wind energy is now one of the fastest growing and attractive renewable energies. The increasing price-competitiveness of wind energy against other conventional fossil fuel energy sources such as coal and natural gas is another positive. WECS consists of three major aspects; aerodynamic, mechanical and electrical as shown in Fig.1. The electrical aspect of WECS can further be divided into three main components, which are wind turbine generators (WTGs), power electronic converters (PECs) and the utility grid.

A. Wind Turbine Generators

With the consideration to its operation speed and the size of the associated converters, WTGs can be classified into three categories namely:

- Fixed Speed Wind Turbine (FSWT)
- Variable Speed Wind Turbine (VSWT) with partial scale frequency converter (PSFC)

- Variable Speed Wind Turbine (VSWT) with full scale frequency converter (FSFC)

FSWT including Squirrel-Cage Induction Generator (SCIG), led the market until 2003. The Doubly-Fed Induction Generator (DFIG), which is the main concept of VSWT with PSFC, overtook FSWT and has been leading WTG concept. It nearly has 85% of the market share.

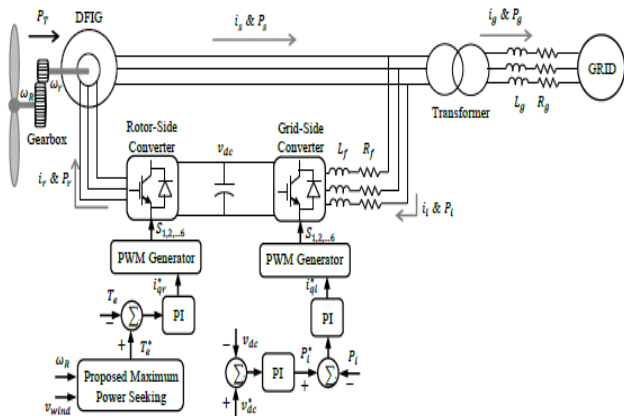


Fig.1. Schematic of a DFIG based wind turbine system.

B. Variable Speed Wind Turbines

almost a constant speed, which is determined by the gear ratio, the grid frequency, and the number of poles of the generator. The maximum conversion efficiency can be achieved only at a given wind speed, and the system efficiency degrades at other wind speeds. The turbine is protected by aerodynamic control of the blades from possible damage caused by high wind gusts. The fixed-speed turbine generates highly fluctuating output power to the grid, causing disturbances to the power system. This type of turbine also requires a sturdy mechanical design to absorb high mechanical stresses. On the other hand, variable-speed wind turbines can achieve maximum energy conversion efficiency over a wide range of wind speeds. The turbine can continuously adjust its rotational speed according to the wind speed. In doing so, the tip speed ratio, which is the ratio of the blade tip speed to the wind speed, can be kept at an optimal value to achieve the maximum power conversion efficiency at different wind speeds. To make the turbine speed adjustable, the wind turbine generator is normally connected to the utility grid through a power converter system. The converter system enables the control of the speed of the generator that is mechanically coupled to the rotor (blades) of the wind turbine. The main advantages of the variable-speed turbine include increased wind energy

output, improved power quality, and reduced mechanical stress. The main drawbacks are the increased manufacturing cost and power losses due to the use of power converters. Nevertheless, the additional cost and power losses are compensated for by the higher energy production. Furthermore, the smoother operation provided by the controlled generator reduces mechanical stress on the turbine, the drive train and the supporting structure. This has enabled manufacturers to develop larger wind turbines that are more cost-effective. Due to the above reasons, variable-speed turbines dominate the present market.

II. TOPOLOGIES OF DFIG

The Doubly-fed induction generator's are mostly utilizes slip ring induction generator. Recently, brushless DFIG are also investigated.

A. Slip Ring Induction Generator

This topology is also called the DFIG. As shown in Fig.2, Its stator circuit is directly connected to the grid while the rotor circuit is connected to grid via slip rings and three-phase converter. The DFIG is currently the system of choice for multi-MW wind turbines. The aerodynamic system must be capable of operating over a wide wind speed range in order to achieve optimum aerodynamic efficiency by tracking the optimum tip-speed ratio. Therefore, the generator's rotor must be able to operate at a variable rotational speed. The DFIG system therefore operates in both sub- and super-synchronous modes with a rotor speed range around the synchronous speed. For variable-speed systems where the speed range requirements are small, for example $\pm 30\%$ of synchronous speed, the DFIG offers adequate performance and is sufficient for the speed range required to exploit typical wind resources. An AC-DC-AC converter is included in the induction generator rotor circuit. The power electronic converters need only be rated to handle a fraction of the total power – the rotor power – typically about 30% nominal generator power. Therefore, the losses in the power electronic converter can be reduced, compared to a system where the converter has to handle the entire power, and the system cost is lower due to the partially-rated power electronics. Here we will introduce the basic features and normal operation of DFIG systems for wind power applications basing the description on the standard induction generator. Different aspects that will be described include their variable-speed feature, power converters and their associated control systems, and application issues.

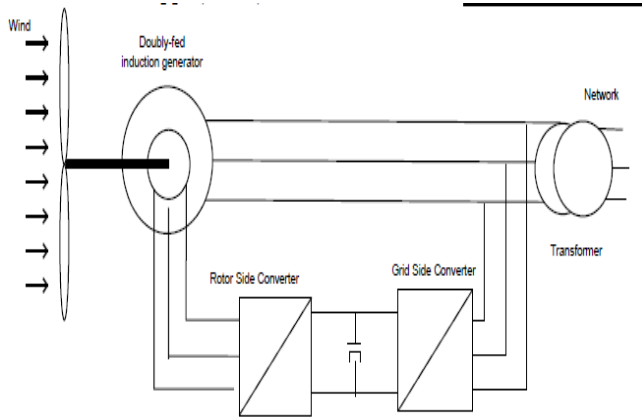


Fig.2. Doubly-fed induction generator

Fig.3. shows mechanical power „P_m“ versus slip, „s“ characteristics of a DFIG wind energy system. The negative value of mechanical power indicates that the DFIG is in the generating mode. Since the rotor speed of the DFIG is adjustable, by using the maximum power point tracking (MPPT) schemes which can be implemented to harvest the maximum available power from the wind turbine. When operating at the maximum power point (MPP) on the turbine power-speed curves, the generator's mechanical power from the shaft „P_m“ is proportional to the cube of the rotor speed „ω_r“. The rotor speed is varying in the range of 0.5 ω_s to 1.2 ω_s. Depending on the rotor speed, there are two modes of operation in a DFIG WECS, namely super-synchronous mode, sub synchronous mode. The slip is negative in the super-synchronous mode and becomes positive in the sub-synchronous mode. Fig.4 and Fig.5 show the power flow in a DFIG during super-synchronous & sub-synchronous mode of operation. Depending on whether the slip is positive or negative, the rotor circuit can receive or deliver power from or to the grid. In the super-synchronous operation mode, the mechanical power |P_m| from the shaft is delivered to the grid through both stator and rotor circuits. The rotor power |P_r| is transferred to the grid by power converters in the rotor circuit, whereas the stator power |P_s| is delivered to the grid directly. Neglecting the losses in the generator and converters, the power delivered to the grid |P_g| is

1.2 ω_s. This speed range is normally sufficient for a wind energy system since the power generated at 42% of the rated speed is 7.4% of the rated power. Dynamically, the DFIG may operate at 30% above the synchronous speed. As a consequence, the power converters in the rotor circuit should be designed to handle about 30% of the rated stator power.

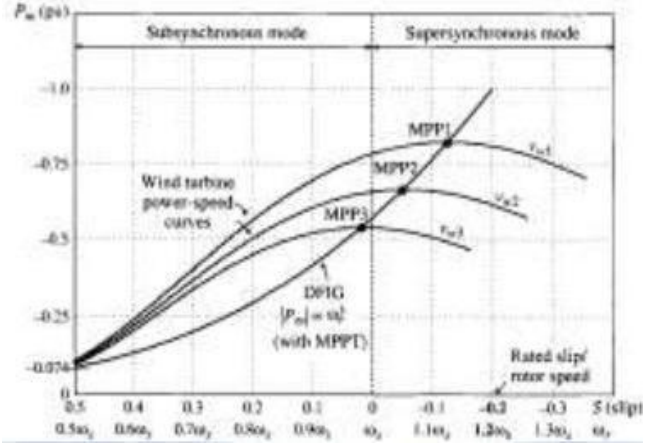


Fig.3. Power-Speed characteristics in a DFIG wind energy system with MPPT control.

the mechanical power |P_m| of the generator, as illustrated in

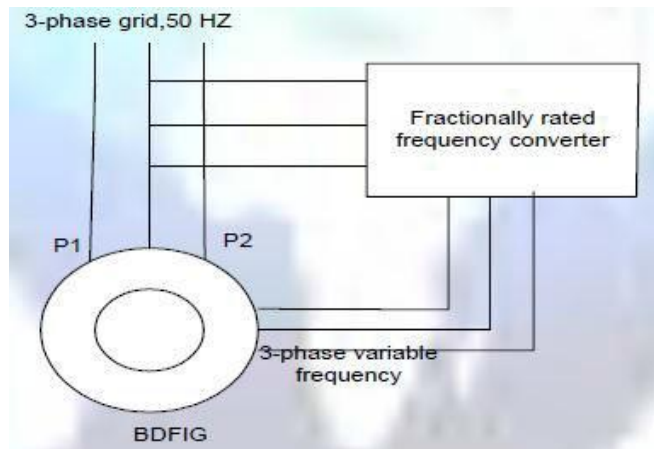


Fig.6. Brushless doubly-fed induction machine connected to the grid

The BDFIG may be thought of as the combination two induction machines, of different stator pole, these machines

will have different synchronous speeds, for the same supply frequency. With their rotors connected together both physically and electrically. Physically this machine is very similar to the self-cascaded machine proposed by Hunt; the main distinction is that the BDFIG is explicitly a doubly-fed machine. This combination of induction machines is similar to the traditional cascade connection of induction machines. In a traditional cascade connection, the rotor of one machine was connected to the stator of the other via slip rings. However it was Hunt realized that if both machines were in the same frame, then rotor can be connected together using slip rings. It can be operated in asynchronous or synchronous mode of operation. During the asynchronous mode of operation, the shaft speed is dependent on the loading of the generator, as well as the supply frequency. If stator 1 has p_1 pole pairs, and stator 2 p_2 pole pairs, then the BDFIG can be operated as an induction generator of either p_1 pole pairs or p_2 pole pairs, by connecting stator 1 or stator 2 respectively.

IV . PROPOSED METHOD FOR MAXIMUM POWER SEEKING

In the proposed technique, three control loops/laws are implemented to (i) determine the desired electrical/generator torque, T_e^* , in the DFIG, as shown in Figure (ii) estimate the wind turbine power capture

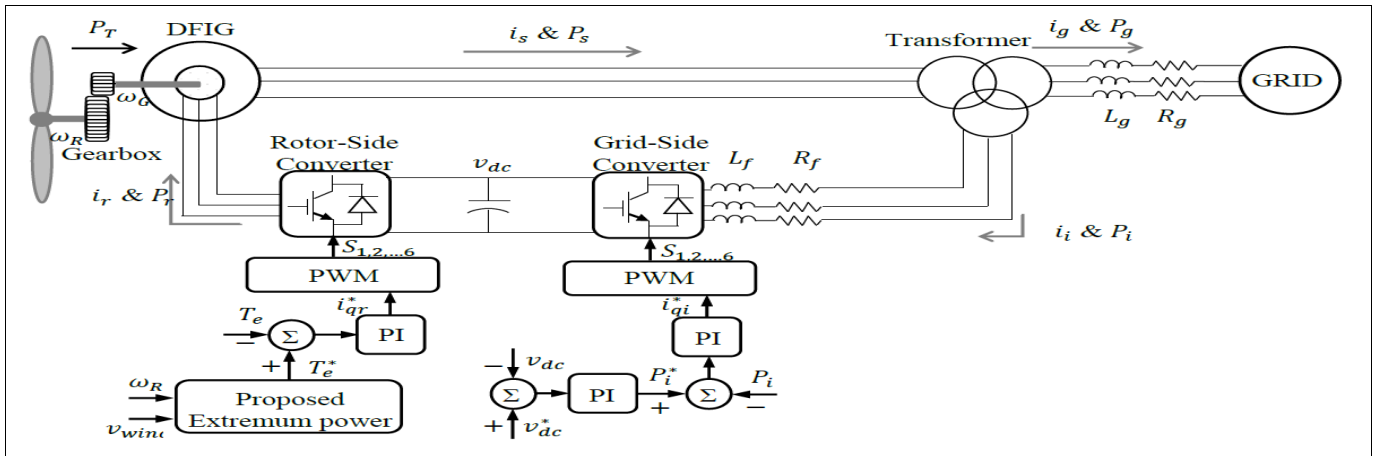


Fig7. Schematic of a DFIG based wind turbine system

can be estimated then the nonlinearity of the equation of motion can be approximately cancelled using the control law

Determine the desired electrical/generator torque, T_e^*

As explained in the previous section, feedback linearization implements a feedback loop in order to transform the nonlinear system into an equivalent linear system by changing the control input signal. As discussed in Chapter 2, aerodynamic or mechanical torque is the nonlinear term of the equation of motion in wind turbines. If the aerodynamic torque

$$T_e^* = \hat{C}_p f(v, \omega_R) - u(t)$$

where

\hat{C}_p is the estimated value of the power capture coefficient and $f(v, \omega_R) = (\rho A v^3 / 2 \omega_R) \propto \omega_R^2$ as defined in Chapter 2. The strategy is to make T_e follows the desired value, T_e^* , resulting in a linear input-output dynamic behavior for the

equation of motion (i.e. $J\dot{\omega}_R + C_D\omega_R = u(t)$). Therefore, the key is to estimate the power coefficient, as explained in the next subsection.

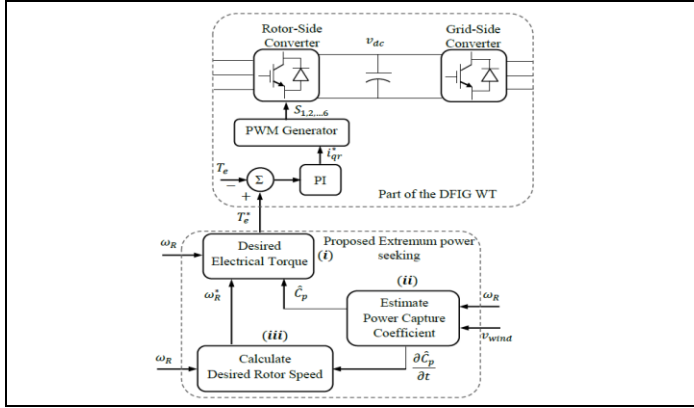


Fig8. Block diagram of the proposed control scheme for extremum power seeking in DFIG-based wind turbines, including (i) desired electrical torque calculator, (ii) power capture coefficient, estimator, and (iii) a desired rotor speed, calculator

Estimation of Power Capture Coefficient, \hat{C}_p through Lyapunov Approach

Estimation of the power capture coefficient, C_p , is used herein for maximizing power capturing. From the equation

$$C_p = \frac{P_T}{P_{avail}} = \frac{P_T}{(1/2)\rho A v^3}$$

where parameters are defined in Chapter 2, the C_p value can be calculated using rotor power or torque measurements; however, the torque measurement requires an additional sensor. Therefore, the common approach is to estimate the torque indirectly via the generator power measurement. In this work, the estimation of C_p is achieved using a Lyapunov-based method. The candidate Lyapunov function, V , is chosen as discussed earlier,

$$V = \frac{1}{2}J\tilde{\omega}_R^2 + \frac{1}{2}\gamma\tilde{C}_p^2$$

where γ is a constant to be determined, $\tilde{\omega}_R = \omega_R^* - \omega_R$ and $\tilde{C}_p = C_p^* - \hat{C}_p$, in which C_p^* is the maximum value of C_p . Computing the time derivative of yields

$$\dot{V} = J\tilde{\omega}_R\dot{\tilde{\omega}}_R + \gamma\tilde{C}_p\dot{\tilde{C}}_p$$

Applying $\dot{\tilde{\omega}}_R = \dot{\omega}_R^* - \dot{\omega}_R$ and $\dot{\tilde{C}}_p = \dot{C}_p^* - \dot{\hat{C}}_p$ yields

$$\dot{V} = J\tilde{\omega}_R(\dot{\omega}_R^* - \dot{\omega}_R) + \gamma\tilde{C}_p(\dot{C}_p^* - \dot{\hat{C}}_p)$$

Neglecting the viscous damping torque, $C_D\omega_R$, of the overall system, and then substituting $\dot{\omega}_R$ from the equation of motion yields

$$\dot{V} = J\tilde{\omega}_R\left(\dot{\omega}_R^* - \frac{1}{J}(T_{aero} - T_e)\right) + \gamma\tilde{C}_p(\dot{C}_p^* - \dot{\hat{C}}_p)$$

Which can be simplified by substituting $T_{aero} = f(v, \omega_R)C_p(\lambda, \beta)$ and T_e from equations

$$\dot{V} = J\tilde{\omega}_R\dot{\omega}_R^* - \tilde{\omega}_R(C_p f - \hat{C}_p f + u) + \gamma\tilde{C}_p(\dot{C}_p^* - \dot{\hat{C}}_p)$$

C_p^* is chosen to be Betz constant (i.e. desired value of power capture coefficient is to be chosen as Betz constant). So, differentiation of C_p^* results 0. Therefore the above equation can be rewritten as

$$\dot{V} = J\tilde{\omega}_R\dot{\omega}_R^* - \tilde{\omega}_R(C_p f - \hat{C}_p f + u) - \gamma\tilde{C}_p\dot{\hat{C}}_p$$

Substituting $\tilde{C}_p = C_p^* - \hat{C}_p$ in equation(4.3.8), yields

$$\dot{V} = J\tilde{\omega}_R \dot{\omega}_R^* - \tilde{\omega}_R (C_p f - \hat{C}_p f + u) - \gamma \dot{\hat{C}}_p (C_p^* - \hat{C}_p)$$

The above equation can be rewritten

$$\dot{V} = \hat{C}_p (\tilde{\omega}_R f + \gamma \dot{\hat{C}}_p) - \tilde{\omega}_R u + J\tilde{\omega}_R \dot{\omega}_R^* - \tilde{\omega}_R C_p f - \gamma \dot{\hat{C}}_p C_p^*$$

The strategy is to make \dot{V} a non-positive quantity. So, the first term in equation is chosen to be zero, that is,

$$\hat{C}_p (\tilde{\omega}_R f + \gamma \dot{\hat{C}}_p) = 0$$

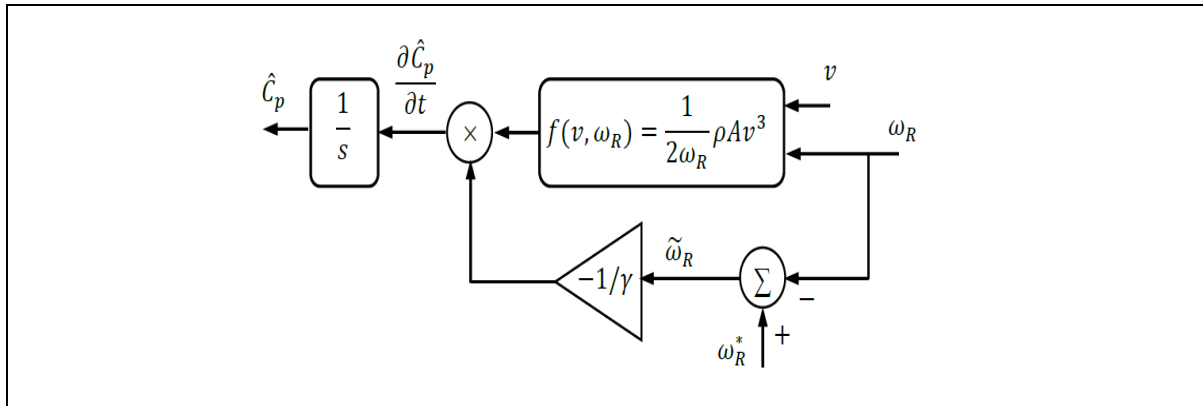
Therefore the derivative of Lyapunov function, i.e. is simplified as

$$\dot{V} = -\tilde{\omega}_R u + J\tilde{\omega}_R \dot{\omega}_R^* - \tilde{\omega}_R C_p f - \gamma \dot{\hat{C}}_p C_p^*$$

Herein, \hat{C}_p is not always equal to zero; therefore, the term in the parenthesis must be zero, resulting in the following differential equation

$$\dot{\hat{C}}_p = -\frac{1}{\gamma} \tilde{\omega}_R f(v, \omega_R)$$

the solution of which provides the estimated power capture coefficient (Figure). In order to keep the second term on the right in (4.3.10) a non-positive value, the control input can be chosen as $u(t) = k_p \omega_R$.



Substituting equation in above equation yields

Fig.9 Estimation of wind turbine power coefficient

$$T_e^* = -\frac{1}{\gamma} f(v, \omega_R) \int \tilde{\omega}_R f(v, \omega_R) dt - k_p \omega_R$$

Therefore, the main control law in (4.3.1) can be rewritten as in equation (4.3.14).

(4.3.1)⇒

$$T_e^* = \hat{C}_p f(v, \omega_R) - u(t)$$

$$T_e^* = \left(\int \dot{\hat{C}}_p dt \right) f(v, \omega_R) - k_p \omega_R$$

The torque control scheme including the feedback linearization loop and the power capture coefficient estimation is shown in Figure .The result can be written as an adaptive PI controller with two time varying parameters:

$$T_e^* = -k_{I1}(t) \int \tilde{\omega}_R k_{I2}(t) dt - k_p \omega_R$$

Maximum Power Seeking Strategy

Where $k_{I1}(t)$ and k_{I2} are time varying parameters.

The maximum-seeking law can also be extracted from the Lyapunov function. Substitution of $u(t) = k_p \tilde{\omega}_R$ and \dot{C}_p^* from (4.3.13) in (4.3.12)

$$\begin{aligned}
 (4.3.12) \quad &\Rightarrow \dot{V} = -\tilde{\omega}_R u + J\tilde{\omega}_R \dot{\omega}_R^* - \tilde{\omega}_R C_p f - \gamma \dot{C}_p C_p^* \\
 &\Rightarrow \dot{V} = -\tilde{\omega}_R k_p \tilde{\omega}_R + J\tilde{\omega}_R \dot{\omega}_R^* - \tilde{\omega}_R C_p f - \gamma \left(-\frac{1}{\gamma} \tilde{\omega}_R f(v, \omega_R) \right) C_p^* \\
 &\Rightarrow \dot{V} = -\tilde{\omega}_R^2 k_p + J\tilde{\omega}_R \dot{\omega}_R^* - \tilde{\omega}_R C_p f + \tilde{\omega}_R f(v, \omega_R) C_p^* \\
 &\Rightarrow \dot{V} = -\tilde{\omega}_R^2 k_p + J\tilde{\omega}_R \dot{\omega}_R^* + (C_p^* - C_p) \tilde{\omega}_R f
 \end{aligned}$$

In the following, $\dot{\omega}_R^*$ is identified to ensure that (4.3.16) is always a non-positive value. In order to hold $\dot{V} \leq 0$, one can choose $\dot{\omega}_R^* \propto (-\tilde{\omega}_R)$ and select k_p adequately large that the first term holds a sufficiently large negative value with respect to the third term as shown in the results demonstrated in next sections. Because $\dot{C}_p^* \propto (-\tilde{\omega}_R)$ and by choosing $\dot{\omega}_R^* \propto (-\tilde{\omega}_R)$, the desired rotor speed can be formulated as

$$\dot{\omega}_R^* = k \dot{C}_p^*$$

This is consistent with the fact that the maximum value of $C_p = P_T / P_{avail}$ and captured power, P_T for a constant wind speed occurs at the same point at which $(\partial P_T / \partial \omega_R) = 0$, as shown in Chapter 2. In the hill-climbing and perturb-and-observe techniques, maximum power is sought according to the sign of $\partial P_T / \partial \omega_R$ such that if the wind turbine operating

V. SIMULATION RESULTS

point is on the left side of the maximum point of the power curve, the desired rotor speed must be increased; if it is on the right side of the maximum point, then the rotor speed must be decreased. The forgoing discussion is valid for a constant or a slowly varying wind speed case. However, if the wind speed suddenly changes, two scenarios are possible:

- wind speed increases thus, $\dot{\omega}_R > 0$ and $P_T > 0$, or
- wind speed decreases thus, $\dot{\omega}_R < 0$ and $P_T > 0$.

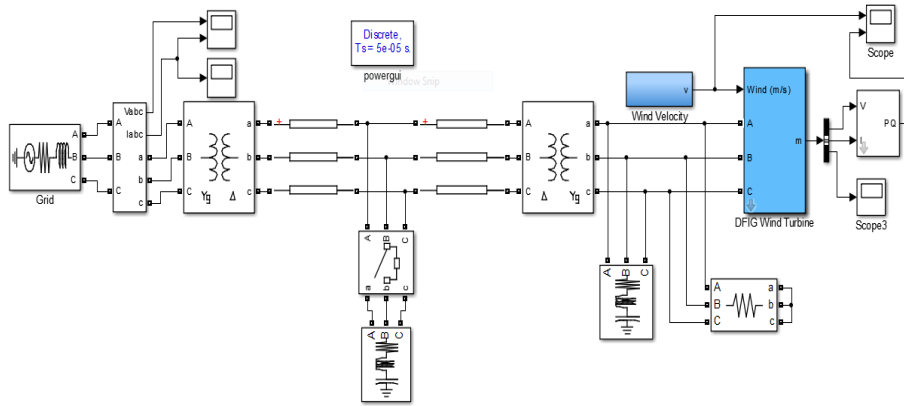


Fig.10. Simulation Block Diagram

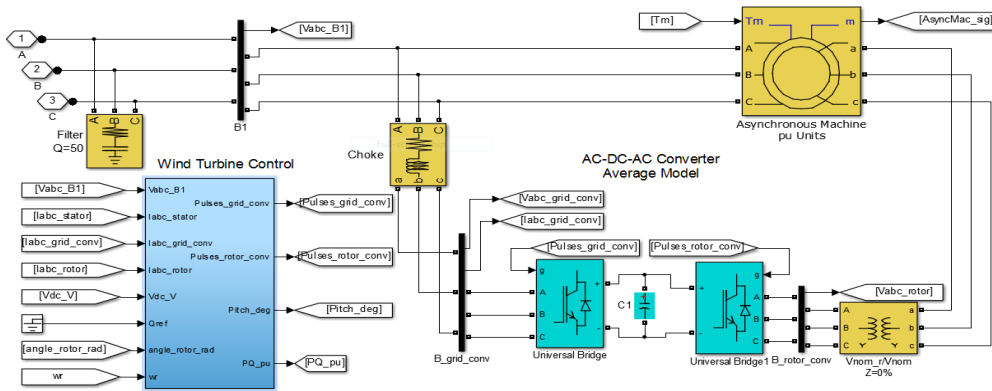


Fig 11. Simulink Block of Wind Turbine

Simulation Block of Proposed Control Technique

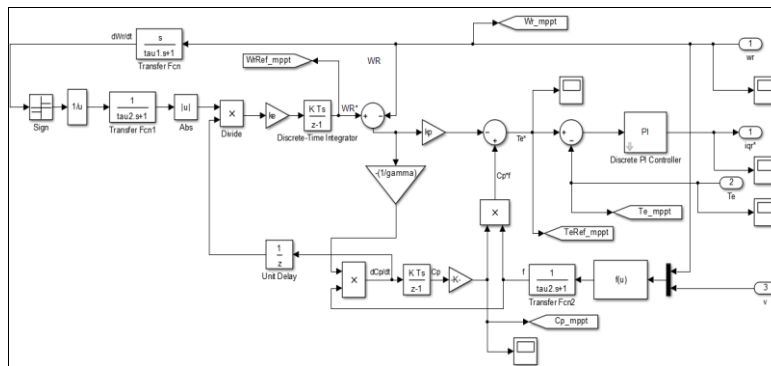


Figure 12. Simulink Block of Control Circuit

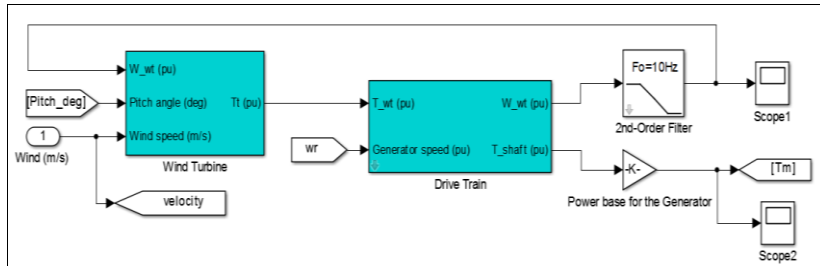


Figure 13. Turbine and Drivetrain

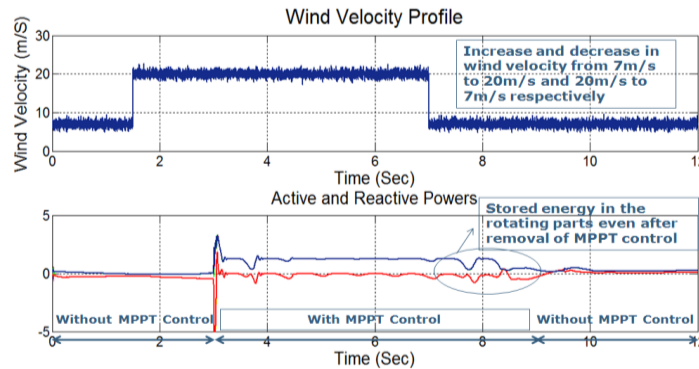


Figure 14. Wind Profile, Active and Reactive Power Changes

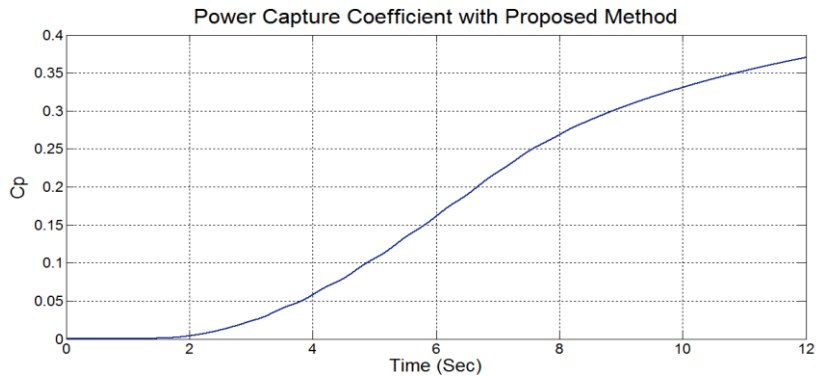
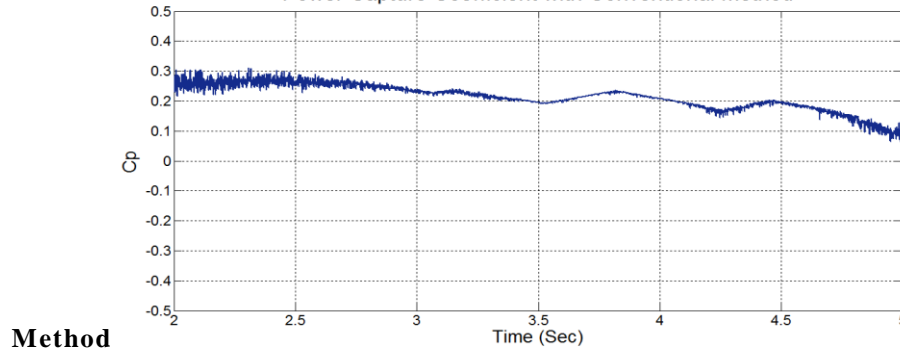


Figure 15. Power Capture Coefficient with the Proposed
 Power Capture Coefficient with Conventional Method



Method

Figure 16. Power Capture Coefficient with the Conventional Method

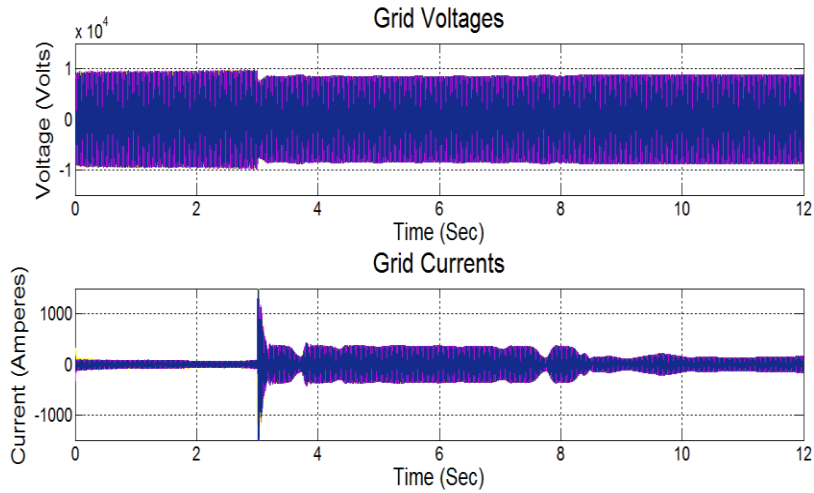


Figure 17. Grid side Voltages and Currents

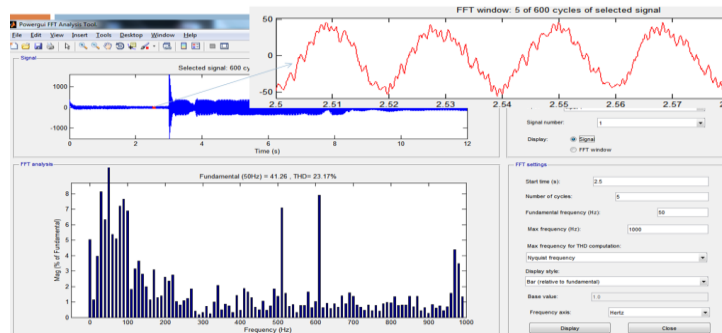


Figure 18. Grid Side Currents Without MPPT Control

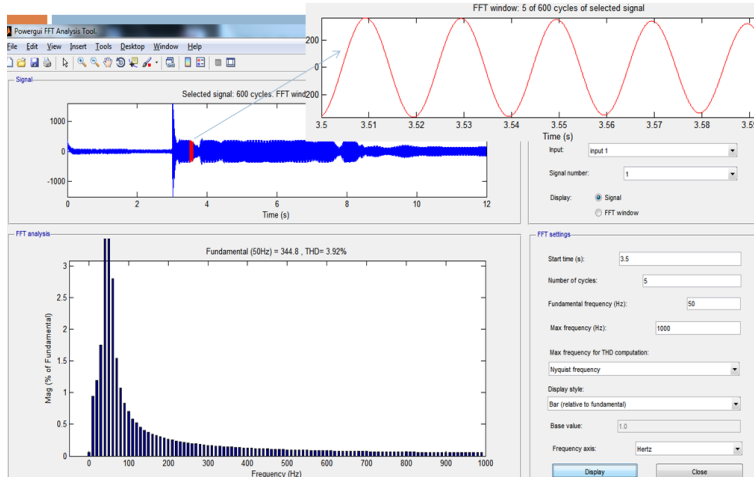


Figure 19. Grid Side Currents With MPPT Control

VI. CONCLUSION
 ANVESHANA'S INTERNATIONAL JOURNAL RESEARCH IN ENGINEERING AND APPLIED SCIENCES

Email Id: anveshanaindia@gmail.com, Website: www.anveshanaindia.com



An adaptive nonlinear control scheme for DFIG-based wind turbines was developed using a Lyapunov-based analysis and feedback linearization. The control scheme was built from three control laws including (i) determining the desired generator torque, (ii) estimating the wind turbine power capture coefficient, and, (iii) calculating the desired rotor speed at which the wind turbine captures maximum available wind power. The control scheme adaptively estimated the wind power capture coefficient using real-time wind and rotor speed values. This control system was developed in the Matlab/Simulink environment, and the overall system was simulated using the 1.5MW DFIG Turbine with back-to-back converters, and a transmission line between the DFIG and the power grid. The two main control schemes (i.e., power capture coefficient estimation with rotor speed regulation and desired rotor speed calculation based on maximizing the estimated power capture coefficient), showed robust dynamic behaviors. The role of the controller is to adaptively reach the maximum power capture coefficient as wind speed changes. The significance of the presented technique compared to existing methods is that neither the maximum power capture coefficient, nor the optimum tip-speed ratio was assumed as a known parameter. Moreover, the presented technique demonstrated a robust dynamic performance in the presence of wind turbulence and sudden speed changes.

Maximum power capturing in variable speed wind turbines is commonly performed in Region 2, as described in dissertation. In Region 3, as wind speed increases, the accelerating torque and rotor speed increases. Therefore, the control strategy in Region 3 regulates power capture at the generator nominal power. During transition between Region 2 and 3, a compensation torque command fed to generator to suppress rotor speed overshoot. Several methods have been reported in the literature, but an optimal nonlinear control scheme that can provide a seamless transition between Region 2 and 3 with minimum stress on the drivetrain is a challenging task as a recommended future work.

VI. REFERENCES

- [1] B. Dudley, "BP energy outlook 2035," British Petroleum, London, United Kingdom, Jan 2014.
- [2] "http://www2.epa.gov/energy/learn-about-energy-and-environment," United States Environmental Protection Agency, 8 Oct 2015. [Online]. Available: <http://www2.epa.gov/energy/learn-about-energy-and-environment>. [Accessed 18 Oct 2015].
- [3] B. Beltran, T. Ahmed-Ali, M. E. H. Benbouzid (2006), "Sliding Mode Power Control of Variable-Speed Wind Energy Conversion Systems," *IEEE Transactions on Energy Conversion* Vol. 23, No. 2, June 2006.
- [4] A. Betz (1926), "Wind Energy and its Exploitation by Windmills," Gottingen: Van-den-hoeck und Ruprecht, p. 64.
- [5] F. Blaabjerg and K. Ma, "Future on power electronics for wind turbine systems," *IEEE Journal of Emerging and selected topics in power electronics*, vol. 1, no. 3, pp. 139 - 152, Sep. 2013.
- [6] M. Malinowski, A. Milczarek, R. Kot, Z. Goryca and J. T. Szuster, "Optimized energy conversion systems for small wind turbines," *IEEE Power Electronics Magazine*, vol. 2, no. 3, pp. 16-30, Sep 2015.
- [7] I. P. Girsang, J. S. Dhupia, E. Muljadi, M. Singh and J. Jonkman, "Modeling and control to mitigate resonant load in variable-speed wind turbine drivetrain," *IEEE Journal of Emerging and Selected Topics in Power Electronics*, vol. 1, no. 4, pp. 277 - 286, 2013.
- [8] B. Connor and W. Leithead, "Control of variable speed wind turbines: Design task," *International Journal of Control*, vol. 73, no. 13, pp. 1189-1212, 2000.
- [9] K. E. Johnson, L. J. Fingersh, M. J. Balas and L. Y. Pao, "Methods for increasing region 2 variable-speed wind turbine," *Journal of Solar Eng*, vol. 126, pp. 1092-1100, 2004.
- [10] L. Y. Pao and K. E. Johnson, "A tutorial on the dynamics and control of wind turbines and wind farms," in *American Control Conference*, St. Louis, 2009.
- [11] M. A. Abdullah, A. M. Yatim, C. W. Tan and R. Saidur, "A review of maximum power point tracking algorithms for wind energy systems," *Renewable and Sustainable Energy Reviews*, vol. 16, pp. 3220-3227, 2012.
- [12] F. Fateh, W. N. White and D. Gruenbacher, "A nonlinear control scheme for extremum power seeking in wind turbine energy conversion systems," in *American Control Conference*, Portland, Oregon, June 2014.
- [13] F. Fateh, W. N. White and D. Gruenbacher, "A maximum power tracking technique for grid-connected DFIG-based wind turbines," *IEEE Journal of Emerging and Selected*



- Topics in Power Electronics*, vol. pp, no. 99, pp. 1-9, 2015.
- [14] F. Fateh, W. White and D. Gruenbacher, "Mitigation of torsional vibrations in the drivetrain of DFIG-based grid-connected wind turbine," in *IEEE Energy Conversion Congress & Exposition*, Montreal, Quebec, Sep 2015.
- [15] S. Musunuri and H. L. Ginn, "Comprehensive review of wind energy maximum power extraction algorithms," in *IEEE Power and Energy Society General Meeting*, San Diego, CA, 2011.
- [16] T. Hawkins, W. N. White, G. Hu and F. D. Sahneh, "Region II wind power capture maximization using robust control and estimation with alternating gradient search," in *American Control Conference*, San Francisco, CA, July 2011.
- [17] A. Ghaffari, M. Krstic and S. Seshagiri, "Power optimization and control in wind energy conversion systems using extremum seeking," *IEEE Transactions on Energy Conversion*, vol. 22, no. 5, pp. 1684-1695, Sep. 2014.
- [18] R. Chedid, S. Karaki and C. El-Chamali, "Adaptive fuzzy control for wind-diesel weak power systems," *IEEE Transactions on Energy Conversion*, vol. 15, no. 1, pp. 71-78, 2000.
- [19] M. g. Simoes, B. K. Bose and R. J. Spiegel, "Fuzzy logic based intelligent control of a variable speed cage machine wind generation system," *IEEE Transactions on Power Electronics*, vol. 12, no. 1, pp. 87-95, 1997.
- [20] H. Li, K. L. Shi and P. McLaren, "Neural network based sensorless maximum wind energy capture with compensated power coefficient," *IEEE Transactions on Industrial Application*, vol. 41, no. 6, pp. 2600-2608, Dec 2005.
- [21] M. Pucci and M. Cirrincione, "Neural MPPT control of wind generators with induction machines without speed sensors," *IEEE Transactions on Industrial Electronics*, vol. 58, no. 1, pp. 37-47, Jan 2011.
- [22] Q. Chen, Y. Li, Z. Yang, J. Seem and J. Creaby, "Self-optimizing-robust control of wind power generation with doubly-fed induction generator," in *IEEE Conference Dynamic Systems and Control*, Cambridge, MA, Sep 2010.
- [23] B. Boukhezzar and H. Siguerdidjane, "Nonlinear control of a variable-speed wind turbine using a two-mass model," *IEEE Transactions on Energy Conversion*, vol. 26, no. 1, pp. 149-162, March 2011.
- [24] E. Iyasere, M. Salah, D. Dawson, J. Wagner and E. Tatlicioglu, "Optimum seeking-based non-linear controller to maximise energy capture in a variable speed wind turbine," *IET Control Theory & Application*, vol. 6, no. 4, pp. 526-532, 2012.
- [25] B. Beltran, T. Ahmed-Ali and M. Benbouzid, "High order sliding –mode control of variable-speed wind turbines," *IEEE Transactions on Industrial Electronics*, vol. 56, no. 9, pp. 3314-3321, Sep 2009.
- [26] L. D. Guerra, F. D. Adegas, J. Stoustrup and M. Monros, "Adaptive control algorithm for improving power capture of wind turbines in turbulent winds.," in *American Control Conference*, Montreal, QC, June 2012.
- [27] G. Mandic, A. Nasiri, E. Muljadi and F. Oyag, "Active torque control for gearbox load reduction in a variable-speed wind turbine," *IEEE Transactions on Industrial Application*, vol. 48, no. 6, pp. 2424-2432, Nov/Dec 2012.